Journal of Power Sources 252 (2014) 58–63

Contents lists available at ScienceDirect

Journal of Power Sources

journal homepage: www.elsevier.com/locate/jpowsour

full-transfer

Symmetrical solid oxide fuel cells with impregnated $SrFe_{0.75}Mo_{0.25}O_{3-\delta}$ electrodes

Xie Meng, Xuejiao Liu, Da Han, Hao Wu, Junliang Li*, Zhongliang Zhan*

CAS Key Laboratory of Materials for Energy Conversion, Shanghai Institute of Ceramics, Chinese Academy of Sciences (SICCAS), 1295 Dingxi Road, Shanghai 200050, China

HIGHLIGHTS

- Nano-scale and symmetrical $SrFe_{0.75}Mo_{0.25}O_{3-\delta}$ electrodes were developed.
- A total polarization resistance of 0.26 Ω cm^2 was achieved at 800 °C.
- Symmetrical fuel cells yielded 0.97 W cm^{-2} in H_2 and 0.39 W cm^{-2} in C_8H_{18} at 800 °C.

ARTICLE INFO

Article history:
Received 9 September 2013
Received in revised form
6 November 2013
Accepted 20 November 2013
Available online 3 December 2013

Keywords:
Solid oxide fuel cells
Strontium and magnesium doped lanthanum gallate
Molybdenum doped strontium ferrite
Nanostructure
Impregnation

ABSTRACT

Here we report nominally symmetrical solid oxide fuel cells that feature thin $La_{0.9}Sr_{0.1}Ga_{0.8}Mg_{0.2}O_{3-\delta}$ (LSGM) electrolytes and impregnated $SrFe_{0.75}Mo_{0.25}O_{3-\delta}$ (SFMO)–LSGM composite electrodes. Operation on hydrogen fuels and air oxidants can produce maximum power densities of 0.39 W cm^{-2} at 650 °C and 0.97 W cm^{-2} at 800 °C. Impedance measurements indicate that the anode and the cathode polarizations are 0.22 and 0.04 Ω cm^2 at 800 °C, respectively. Hydrogen partial pressure and temperature dependence of impedance data in humidified hydrogen shows that hydrogen oxidation kinetics is largely determined by hydrogen adsorption on the SFMO catalysts at high temperatures and charge transfer reactions along the SFMO|LSGM interfaces at low temperatures. Carbon tolerance of the present fuel cells is also examined in *iso*-octane fuels balanced by nitrogen at 800 °C that yields stable maximum power densities of 0.39 W cm^{-2}.

1. Introduction

The current state-of-the-art solid oxide fuel cell (SOFC) typically consists of a dense yttria-stabilized zirconia (YSZ) electrolyte asymmetrically sandwiched between a Ni–YSZ cermet anode and a strontium lanthanum manganite (LSM) cathode, which are respectively exposed to a reducing and oxidizing atmosphere [1,2]. Recently, a novel symmetrical solid oxide fuel cell, where the same material is simultaneously used as the anode and the cathode, has gained increasing interest due to a number of attractive advantages over the common asymmetrical counterpart – such as simplified fabrication procedure, reduced processing costs, minimized compatibility issues, high redox stability as well as enhanced tolerance of the anode toward coking formation and sulphur poisoning [3]. The very different environments for the anode and the cathode pose rather restrictive requirements on the material as the symmetrical fuel cell electrode, including structural stability and acceptable electrical conductivity at the operating temperature in both oxidizing and reducing conditions as well as reasonably high electrochemical activities for oxygen reduction and fuel oxidation reactions [3].

Up to date, only a very limited number of materials can fulfil almost all the conditions required for a symmetrical electrode, and most efforts have been focused upon perovskite oxides due to their wide tunability in their electronic and oxide ion transport behaviour, surface chemistry and catalytic property, as well as chemical and structural stability in both the oxidizing and reducing atmospheres [3,4]. (Sr, Ca)-doped $LaCrO_3$ perovskite oxides were explored as the symmetrical electrode materials due to their well-known stability and acceptable electrical conductivities in both atmospheres demonstrated as the conventional interconnecting materials [5,6]. For example, Sfeir et al. reported a combined anode

* Corresponding authors. Tel./fax: +86 21 6990 6373.
E-mail addresses: ljl2005@mail.sic.ac.cn (J. Li), zzhan@mail.sic.ac.cn (Z. Zhan).

0378-7753/$ – see front matter © 2013 Elsevier B.V. All rights reserved.
http://dx.doi.org/10.1016/j.jpowsour.2013.11.049

and cathode polarization resistance of 0.80 Ω cm^2 and a maximum power density of ≈0.11 W cm^{-2} at 950 °C for fuel cells with thick YSZ electrolytes and symmetrical $La_{0.7}Ca_{0.3}CrO_{3-\delta}$ electrodes, operating on hydrogen fuels and air oxidants. Nevertheless, the catalytic activity of the $La_{0.7}Ca_{0.3}CrO_{3-\delta}$ electrode for methane oxidation was very poor, producing very low power densities of 0.025 W cm^{-2} at 950 °C [7]. In order to enhance the catalytic activity of these chromites for fuel oxidation reactions, Cr was partly substituted by Mn and maximum power densities as high as 0.30 and 0.23 W cm^{-2} were obtained respectively in humidified hydrogen and methane fuels for the resulting symmetrical $La_{0.75}Sr_{0.25}Cr_{0.5}Mn_{0.5}O_{3-\delta}$ electrode fuel cells at 900 °C [8].

Mo-doped $SrFeO_3$ perovskite oxides exhibited good stability and high electrical conductivities in both oxidizing and reducing conditions, and power densities of 0.83 and 0.23 W cm^{-2} were achieved at 900 °C for electrolyte-supported, symmetrical $SrFe_{0.75}Mo_{0.25}O_{3-\delta}$ (SFMO) electrode fuel cells in hydrogen and methane fuels, respectively [9]. Nevertheless, the power densities for such fuel cells became prohibitively small at reduced temperatures due to drastically increased polarization resistances for the micron-scale SFMO electrodes in addition to unacceptably large ohmic resistances for thick electrolytes [9]. Recently, We demonstrated that nano-scale SFMO coatings deposited via the liquid phase infiltration technique onto the internal surfaces of the porous LSGM backbones exhibited much smaller polarization resistances in air than the micron-scale SFMO catalysts, *e.g.*, 0.04 Ω cm^2 for the former versus 0.11 Ω cm^2 for the latter at 800 °C [10]. We also showed that reduced SFMO consisted predominantly of $SrFe_{0.675}Mo_{0.325}O_{3-\delta}$ perovskite oxides and a small portion of metallic Fe that did not increase continuously with extended exposure to hydrogen at 800 °C [11]. In the present paper, the electrochemical characteristics of the nominally symmetrical SFMO electrodes and thin LSGM electrolyte fuel cells were evaluated over the temperature regime of 650–800 °C. The catalytic activities of the nano-scale SFMO–LSGM composites for hydrogen oxidation reactions were investigated in detail, and the tolerance of the reduced SFMO oxides in *iso*-octane fuels was also explored.

2. Experimental

Symmetrical fuel cells with thin LSGM electrolytes were fabricated by first preparing porous|dense|porous LSGM tri-layers, which were produced by laminating three tape-cast ceramic green tapes, with 40 wt% starch filler used as the fugitive material for the two porous layers. The laminated green tapes were co-fired at 1400 °C to produce the final ceramic structures. The addition of the electrode catalysts, $SrFe_{0.75}Mo_{0.25}O_3$ (SFMO), was the next step in the fuel cell fabrication procedure. An aqueous solution containing $Sr(NO_3)_2$, $Fe(NO_3)_3 \cdot 9H_2O$, $(NH_4)_6Mo_7O_{24} \cdot 4H_2O$ and citric acid in a molar ratio of 1:0.75:0.0357:2 was impregnated into the porous LSGM backbones and dried, followed by calcinations at 850 °C for 2 h. The ultimate loadings of the infiltrated catalysts in the porous LSGM layers were controlled by varying the number of impregnation/firing cycles.

The symmetrical fuel cells were tested using a standard geometry at temperatures from 650 °C to 800 °C. Current–voltage curves and electrochemical impedance spectra were obtained using an IM6 Electrochemical Workstation (ZAHNER, Germany) with the cathode exposed to dry air at 100 sccm and the anode to humidified (3% H_2O) hydrogen at 100 sccm, or *iso*-octane bubbled at 25 °C by nitrogen at varied flow rates that produces a mixture of 6% C_8H_{18}–94% N_2. The individual electrode polarization resistances were determined by testing such symmetrical fuel cells in dry air for the cathode polarization resistances and in humidified (3% H_2O) hydrogen for the anode polarization resistances. The impedance data were recorded with a perturbation voltage of 20 mV over the frequency range 0.1 Hz–100 kHz. The cell structure was examined after testing using scanning electron microscopy (SEM) in a Hitachi S-4800-II microscope.

3. Results and discussion

Fig. 1a shows an SEM micrograph of symmetrical fuel cells, which were developed on the basis of an LSGM tri-layer – ≈15 μm thick dense layer sandwiched between two 150 μm thick porous layers. The porous LSGM backbones had a median pore size of 3 μm and an apparent porosity of ≈45% as measured by the Archimedes' method. Fig. 1b shows a higher-magnification micrograph of the impregnated composite electrodes as synthesized at 850 °C in air, showing that the average particle size was ≈70 nm. Higher calcination temperatures above 850 °C were not pursued due to increased particle size and reduced surface area available for electrochemical reactions [10]. As observed previously, these infiltrate coatings consisted predominantly of $SrFe_{0.75}Mo_{0.25}O_{3-\delta}$ with minor $SrMoO_4$ in air and of $SrFe_{0.675}Mo_{0.325}O_{3-\delta}$ with minor metallic Fe in hydrogen [10,11]. Fig. 1b also shows that a solid loading of 25% relative to the porous LSGM backbone was sufficient to form well-interconnect coatings, which is critically important to reducing the ohmic contributions of the porous LSGM backbones to the overall cell resistances.

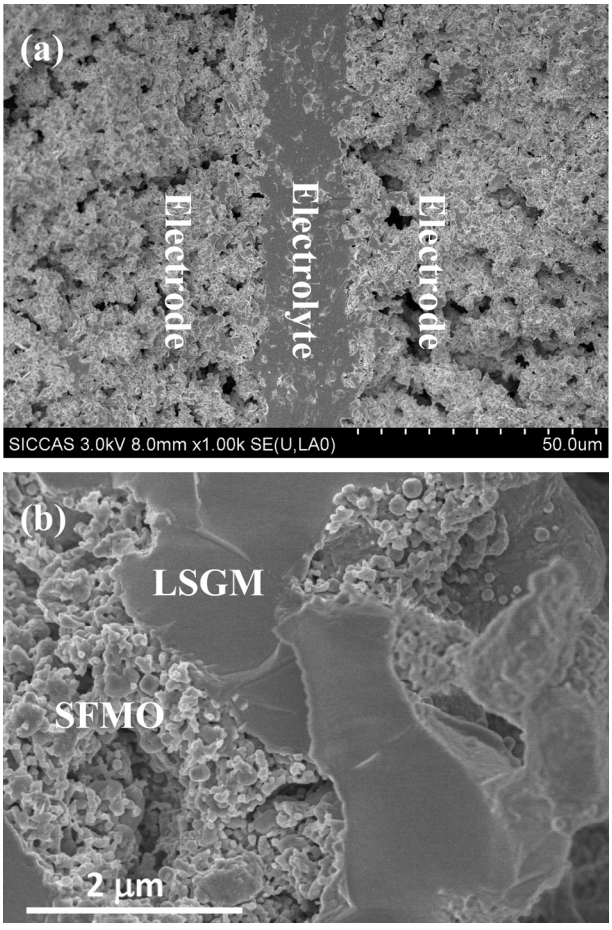

Fig. 1. Cross-sectional SEM images showing a symmetrical and thin LSGM electrolyte fuel cell: (a) a low magnification survey image and (b) a higher magnification view of the electrode.

Electrochemical measurements were performed on the nominally symmetrical fuel cells with humidified hydrogen fuels and dry air oxidants at 650–800 °C. Fig. 2a shows typical cell voltages (V) and power densities (P) as a function of current densities (J). The open circuit voltage (OCV) values ranged between 1.061 and 1.095 V, and were approximately 50 mV smaller than the calculated Nernst potentials due to slight leakage through the ceramic sealing as previously observed [12]. The maximum power densities measured were 0.97, 0.85, 0.60 and 0.39 W cm^{-2} at 800, 750, 700 and 650 °C, respectively. These results compare very favourably with prior symmetrical fuel cells that usually required operating temperatures above 850 °C so as to deliver reasonably high power densities, *e.g.*, 0.64 W cm^{-2} at 850 °C for 265 μm thick LSGM electrolyte fuel cells with symmetrical micron-scale SFMO electrodes [9], 0.55 W cm^{-2} at 950 °C for 250 μm thick YSZ electrolyte fuel cells with symmetrical LSCM–YSZ electrodes [13], or 0.31 W cm^{-2} at 900 °C for 300 μm thick scandium-stabilized zirconia electrolyte fuel cells with symmetrical $La_{0.8}Sr_{0.2}Sc_{0.2}Mn_{0.8}O_{3-\delta}$ electrodes [14]. Note that the J–V curves in Fig. 2 show some evidence of concentration polarization at high current densities, especially at high temperatures. This indicates that the relatively low porosity (typically <30%) of the LSGM backbones after SFMO impregnation might be limiting the fuel cell performance. Therefore, the present symmetrical fuel cells have potentials for further improvement by tailoring the pore structure and increasing the porosity of the LSGM backbones.

Fig. 2b shows Nyquist plots of impedance data obtained at open circuits for the present nominally symmetrical fuel cells, where two depressed arcs were observed at all temperatures. The higher-frequency arc increased exponentially with decreasing temperature, as typically observed for charge transfer reactions or surface diffusions. In contrast, the lower-frequency arc remained almost independent of temperature, which was probably associated with gas transport within the porous structure or gas adsorption on the catalyst surface. The combined anode and cathode interfacial polarization resistances, taken as the overall widths of depressed arcs, were 0.18, 0.22, 0.30 and 0.45 Ω cm^2 at 800, 750, 700 and 650 °C, respectively.

In order to determine the respective polarization resistances of the SFMO–LSGM composites for hydrogen oxidation and oxygen reduction reactions, electrochemical impedance spectroscopy (EIS) measurements were performed on the symmetrical fuel cells that were exposed to a uniform atmosphere of 97% H_2–3% H_2O or dry air. Note that these EIS data should be cautiously correlated with the performance for functional symmetric fuel cells that are exposed to asymmetric gases, but do provide an effective measure of the catalytic activities of the electrodes for the electrochemical reactions. Representative Nyquist plots of the EIS data at 750 °C are shown in Fig. 3a for symmetrical cathode fuel cells in dry air and in Fig. 3b for symmetrical anode fuel cells in humidified hydrogen. The cathode polarization resistance was $R_{P,C} = 0.05$ Ω cm^2, similar

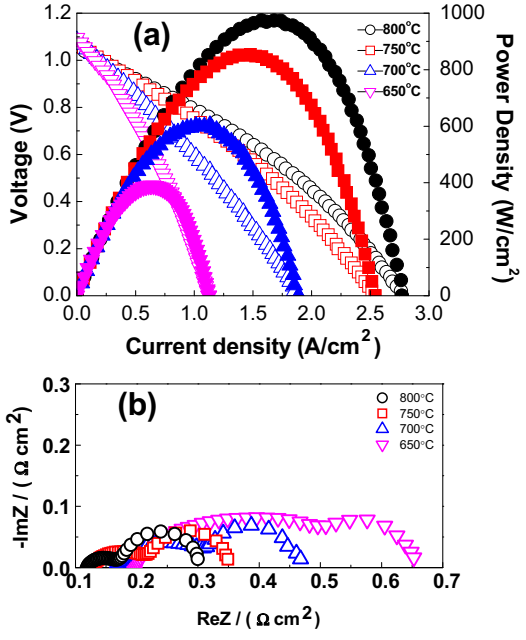

Fig. 2. (a) Voltage and power density versus current density for a symmetrical fuel cell measured in humidified hydrogen fuel and dry air at 100 sccm over the temperature range of 650–800 °C. (b) Nyquist plots of impedance data measured at open circuits.

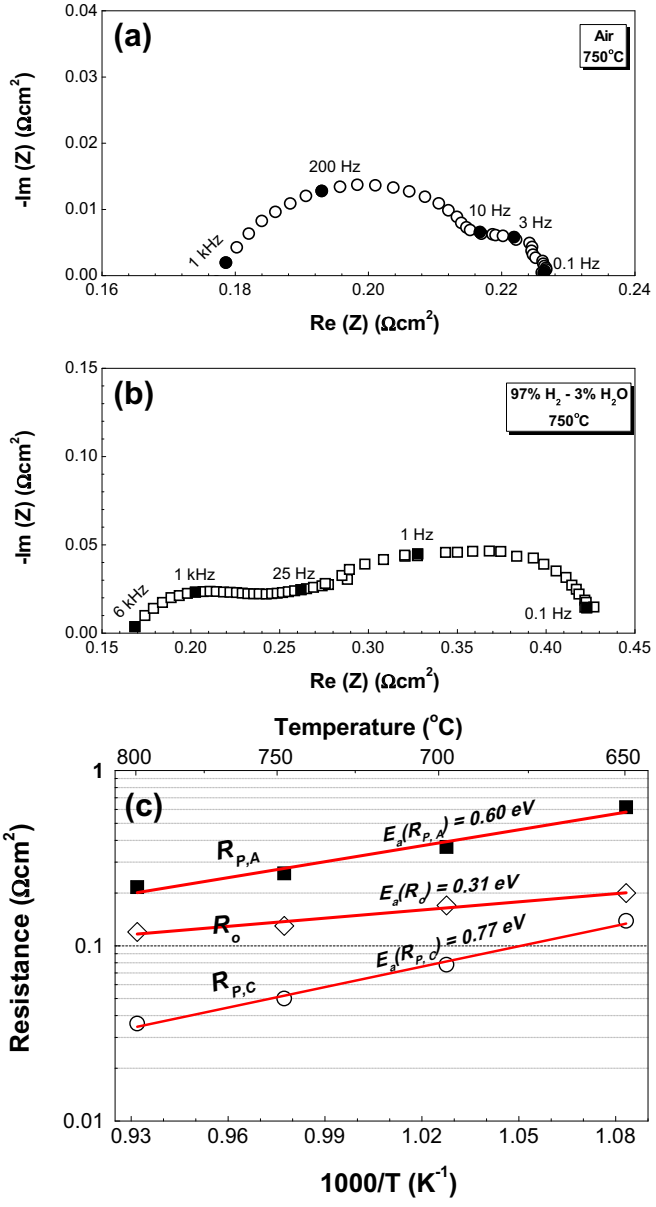

Fig. 3. Representative impedance spectra measured at 750 °C for the symmetrical fuel cell in (a) 97% H_2–3% H_2O and (b) dry air at 100 sccm. (c) The ohmic, anode and cathode polarization resistances plotted versus inverse temperature.

to the value observed for the $La_{0.8}Sr_{0.2}FeO_3$ (LSF) impregnated YSZ composites at the same temperature [15]. Such a small $R_{P,C}$ value also indicated that the presence of minor $SrMoO_4$ impurities in the SFMO coatings did not substantially affect the catalytic activity of impregnated SFMO–LSGM composite for oxygen reduction reactions [10]. Fig. 3b shows that the anode polarization resistance was $R_{P,A} = 0.25\ \Omega\ cm^2$ at 750 °C, which was comparable to values for the commonly used Ni–YSZ cermet anodes that showed $R_{P,A} = 0.1\ \Omega\ cm^2$ under similar conditions [16,17].

The above results indicated that the impregnated SFMO–LSGM composites performed well as the symmetrical electrodes at reduced temperatures. Note that the common micron-scale SFMO electrodes showed much larger polarization resistances under comparable conditions, *e.g.*, $R_{P,A} = 0.45\ \Omega\ cm^2$ in hydrogen and $R_{P,C} = 0.65\ \Omega\ cm^2$ in air at 750 °C [9]. Alternative symmetrical electrodes are required to work at higher temperatures in order to achieve similar catalytic activities and yield comparable polarization resistances, *e.g.*, $R_{P,A} = 0.30\ \Omega\ cm^2$ and $R_{P,C} = 0.18\ \Omega\ cm^2$ at 950 °C for $La_{0.75}Sr_{0.25}Cr_{0.5}Al_{0.5}O_{3-\delta}$ electrodes on the LSGM electrolytes [18], $R_{P,A} = 0.18\ \Omega\ cm^2$ and $R_{P,C} = 0.09\ \Omega\ cm^2$ at 950 °C for LSCM–YSZ electrodes on the YSZ electrolytes [13], $R_{P,A} = 1.4\ \Omega\ cm^2$ and $R_{P,C} = 0.25\ \Omega\ cm^2$ at 800 °C for $La_{0.7}Ca_{0.3}Cr_{0.5}Mn_{0.5}O_{3-\delta}$ electrodes on the YSZ electrolytes [19]. The superior electro-catalytic activities of the present SFMO impregnated LSGM composites can be ascribed to the dramatically increased number of active sites for both hydrogen oxidation and oxygen reduction reactions as well as the important mixed ionic and electronic conducting behaviour of SFMO as enabled by the strong hybridization of the Fe d and O p states [20,21].

The $R_{P,A}$ and $R_{P,C}$ values at varied temperatures are summarized in Fig. 3c together with the ohmic resistances (R_o) as obtained from the high-frequency real-axis intercepts in Fig. 2b, showing that the anode polarization was the dominant loss while the cathode polarization was almost negligibly small. With temperature decreasing from 800 °C to 650 °C, the $R_{P,A}$ value increased from 0.22 Ω cm^2 to 0.62 Ω cm^2, and the $R_{P,C}$ value increased from 0.035 Ω cm^2 to 0.13 Ω cm^2. Note that the ohmic resistances in Fig. 3c were larger than expected values (R_{EL}) for a 15 μm-thick LSGM electrolyte based upon the measured ionic conductivities, *e.g.*, $R_o = 0.13\ \Omega\ cm^2$ versus $R_{EL} = 0.017\ \Omega\ cm^2$ at 750 °C. Given that the current collection losses in the present four-probe testing setup were typically small (~0.03 Ω cm^2) [22], such large differences between R_o and R_{EL} indicate that there were additional contributions from the SFMO–LSGM electrodes due to insufficient electrical conductivities for SFMO catalysts, especially in hydrogen atmospheres [23]. This conclusion was further supported by the observation that a symmetrical fuel cell impregnated with more conductive $Sm_{0.5}Sr_{0.5}CoO_{3-\delta}$ coatings at a similar loading yielded a much smaller ohmic resistance of 0.067 Ω cm^2 at 750 °C [22,24]. These results suggest that optimizing the current collection to compensate the relatively low electrical conductivities of SFMO catalysts would undoubtedly increase the fuel cell power densities.

As shown in Fig. 3a and b, the Nyquist plots in both hydrogen and air consist of two depressed arcs centred at 0.2–2 kHz and 0.4–4 Hz, respectively. Prior reports showed that the higher- and lower-frequency arcs in air are respectively associated with ionization of adsorbed oxygen atom and non-dissociative adsorption of gaseous oxygen on the SFMO catalysts [10]. In order to gain insights into hydrogen oxidation kinetics on the impregnated SFMO–LSGM composites, impedance data for symmetrical anode fuel cells in humidified hydrogen were fitted using the equivalent circuits $LR_o(RQ)_H(RQ)_L$, where L was the conductance due to connecting wires, R_o was the pure ohmic resistance, R_h and R_l were the polarization resistances whereas Q_h and Q_l were the constant phase elements associated with the higher- and lower-frequecy process,

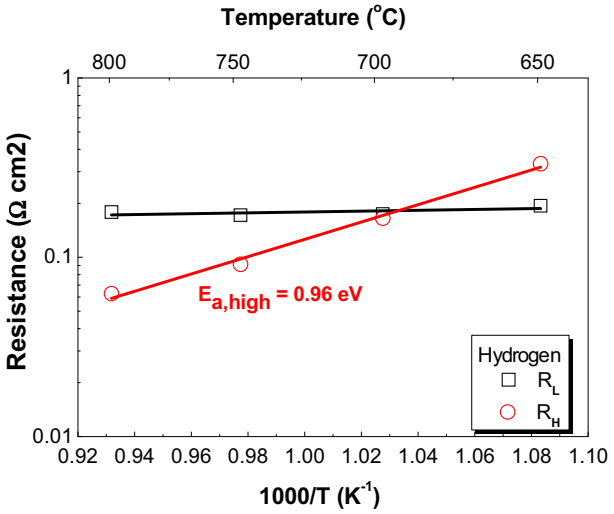

Fig. 4. Temperature dependence of the higher- and lower-frequency arcs for impedance spectra in humidified hydrogen fuels. The equivalent circuits $LR_o(RQ)_H(RQ)_L$ was used to fit the impedance data at varied temperatures.

respectively. Fig. 4 shows the resulting R_h and R_l values as a function of temperature. As previously observed for oxygen reduction on symmetrical cathode fuel cells, the higher-frequency arc for hydrogen oxidation also followed an Arrhenius dependence while the lower-frequency arc remained almost unchanged with temperature. Furthermore, the activation energies for R_H were almost the same, 0.96 ± 0.02 eV for hydrogen oxidation versus 0.98 ± 0.04 eV for oxygen reduction [10]. Therefore, the higher-frequency arc might be correlated with the same physical process occurring in both the anode and the cathode, which is probably the charge transfer reaction along the SFMO/LSGM interfaces [10]. On the other hand, the temperature-independent lower-frequency arc is likely related to hydrogen adsorption on the catalysts. These conclusions were further supported by hydrogen partial pressure dependence of these two arcs as shown in Fig. 5, where the higher-frequency arcs changed little with hydrogen partial pressure and stayed almost constant around 0.13 Ω cm^2 while the lower-frequency arc increased dramatically from 0.15 Ω cm^2 at 1 atm to 0.41 Ω cm^2 at 0.10 atm. Comparison of the R_h and R_l values in Fig. 4 indicates that hydrogen oxidation kinetics on the impregnated

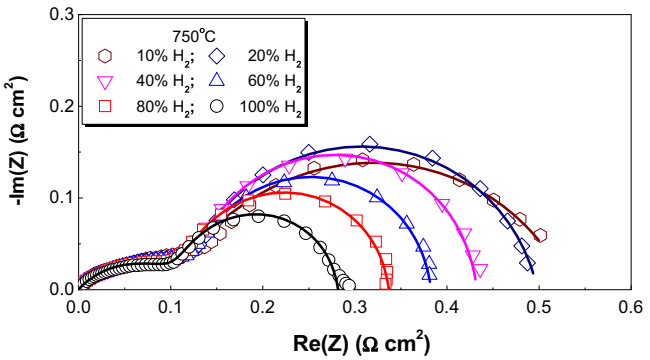

Fig. 5. Nyquist plots of impedance data for the symmetrical fuel cells in humidified hydrogen fuels balanced by nitrogen. The equivalent circuits $LR_o(RQ)_H(RQ)_L$ was used to fit the impedance data at varied hydrogen partial pressures.

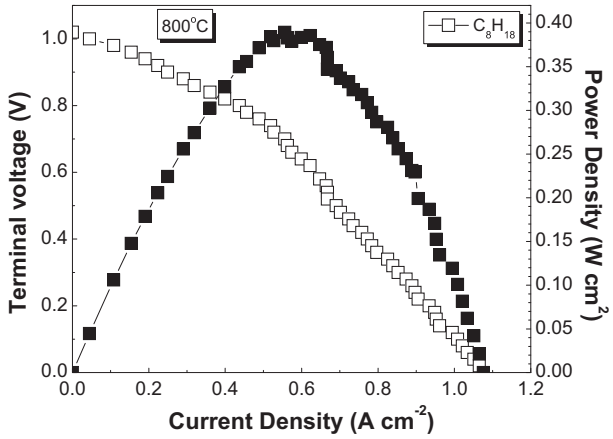

Fig. 6. Voltage and power density versus current density for a symmetrical fuel cell measured at 800 °C in 6% iso-octane fuels balanced by nitrogen at 100 sccm and dry air at 100 sccm.

SFMO–LSGM composites was dominated by hydrogen adsorption at high temperatures and charge transfer at low temperatures.

In order to evaluate the tolerance of the impregnated SFMO–LSGM composites toward coking formation at elevated temperatures, the symmetrical fuel cells were also measured with heavy hydrocarbon fuels. Fig. 6 shows the cell voltages and power densities as a function of current densities for the present fuel cells operating on 6% *iso*-octane balanced by nitrogen at 800 °C. The OCV value was ≈1.0 V and the maximum power density was 0.389 W cm^{-2}, which is comparable to previously reported values for copper–ceria-cermet anode fuel cells operating on propane, dodecane or diesel fuels [12]. Since gas leakage through the sealing was excluded based upon good agreement between the experimentally observed OCV values shown in Fig. 2 and the thermodynamic predictions for hydrogen fuels, the relatively low OCV value for *iso*-octane fuels seemingly indicated that partial oxidation reactions might be substantial in the anodic oxidation process, as previously observed for electrochemical oxidation of propane, butane and diesel on the copper cermet anodes [12,25]. Although extended long-term tests would be more relevant, some preliminary results in Fig. 7 showed that stable power output can be well maintained at a current density of 0.4 A cm^{-2} at 800 °C, which was smaller than in Fig. 6 due to cell-to-cell difference. These

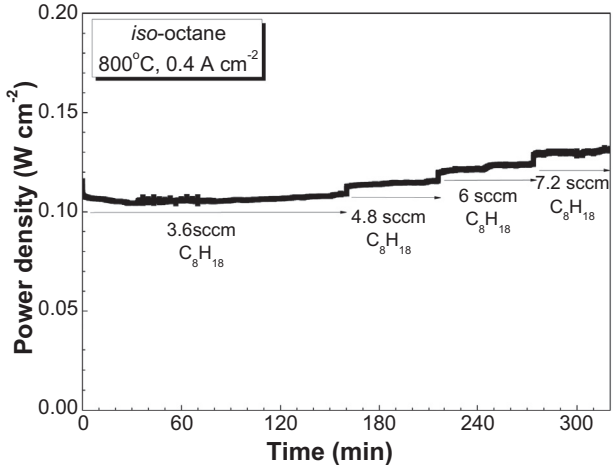

Fig. 7. Stability of the symmetric fuel cell operating at 800 °C on iso-octane fuels and air oxidants.

results demonstrate that the SFMO–LSGM composite electrodes can provide superior resistance toward coking formation at elevated temperatures.

4. Conclusions

In summary, we fabricated nominally symmetrical solid oxide fuel cells that are based upon tri-layer structures of porous|dense|porous LSGM with nano-scale SFMO catalysts simultaneously impregnated onto the internal surfaces of both porous LSGM backbones. Unprecedently high power densities were achieved in hydrogen fuels, *e.g.*, 0.97 W cm^{-2} at 800 °C. Impedance measurements indicated that the resulting SFMO–LSGM composites exhibited larger polarization resistances in hydrogen than in air, *i.e.*, 0.22 versus 0.04 Ω cm^2 at 800 °C. Analysis on hydrogen partial pressure and temperature dependence of impedance data indicated that hydrogen adsorption on the SFMO catalysts and charge transfer reactions along the SFMO|LSGM interfaces were the rate-limiting step for hydrogen oxidation reactions on the impregnated SFMO–LSGM composites at high and low temperatures, respectively. Furthermore, the impregnated SFMO–LSGM composites exhibited good carbon tolerance in *iso*-octane fuels, enabling maximum power densities as high as 0.39 W cm^{-2} at 800 °C.

Acknowledgements

The authors gratefully acknowledge the financial support of the National Basic Research Program of China under contract No. 2012CB215401, the National Science Foundation of China under contract No. 51072219, 51272272, Science and Technology Commission of Shanghai Municipality under contract No. 11PJ1410300, Science and Technology Commission of Zhejiang Province under contract No. 2011C16037, Chinese Government High Tech Developing Project under contract No. 2011AA050702, and the 100 Talents Program of Chinese Academy of Sciences.

References

[1] R.M. Ormerod, Chem. Soc. Rev. 32 (2003) 17–28.
[2] A.J. Jacobson, Chem. Mater. 22 (2010) 660–674.
[3] J.C. Ruiz-Morales, D. Marrero-Lopez, J. Canales-Vazquez, J.T.S. Irvine, RSC Adv. 1 (2011) 1403–1414.
[4] M.A. Pena, J.L.G. Fierro, Chem. Rev. 101 (2001) 1981–2017.
[5] N.Q. Minh, J. Am. Ceram. Soc. 76 (1993) 563–588.
[6] J.C. Ruiz-Morales, H. Lincke, D. Marrero-Lopez, J. Canales-Vazquez, P. Nunez, Bol. Soc. Esp. Ceram. Vidrio 46 (2007) 218–223.
[7] J. Sfeir, P.A. Buffat, P. Mockli, N. Xanthopoulos, R. Vasquez, H.J. Mathieu, J. Van herle, K.R. Thampi, J. Catal. 202 (2001) 229–244.
[8] D.M. Bastidas, S.W. Tao, J.T.S. Irvine, J. Mater. Chem. 16 (2006) 1603–1605.
[9] Q.A. Liu, X.H. Dong, G.L. Xiao, F. Zhao, F.L. Chen, Adv. Mater. 22 (2010) 5478–5482.
[10] X. Meng, D. Han, H. Wu, J.L. Li, Z.L. Zhan, J. Power Sources 246 (2014) 906–911.
[11] Y.C. Zhou, X.J. Liu, X. Pan, J.L. Li, X.F. Ye, H.W. Nie, C.R. Xia, S.R. Wang, Z.L. Zhan, J. Power Sources (2014) submitted for publication.
[12] L. Zhao, X.F. Ye, Z.L. Zhan, J. Power Sources 196 (2011) 6201–6204.
[13] J.C. Ruiz-Morales, J. Canales-Vazquez, J. Pena-Martinez, D. Marrero-Lopez, P. Nunez, Electrochim. Acta 52 (2006) 278–284.
[14] Y. Zheng, C. Zhang, R. Ran, R. Cai, Z.P. Shao, D. Farrusseng, Acta Mater. 57 (2009) 1165–1175.
[15] W.S. Wang, M.D. Gross, J.M. Vohs, R.J. Gorte, J. Electrochem. Soc. 154 (2007) B439–B445.
[16] J.S. Cronin, J.R. Wilson, S.A. Barnett, J. Power Sources 196 (2011) 2640–2643.
[17] J.R. Wilson, W. Kobsiriphat, R. Mendoza, H.Y. Chen, J.M. Hiller, D.J. Miller, K. Thornton, P.W. Voorhees, S.B. Adler, S.A. Barnett, Nat. Mater. 5 (2006) 541–544.
[18] J. Pena-Martinez, D. Marrero-Lopez, D. Perez-Coll, J.C. Ruiz-Morales, P. Nunez, Electrochim. Acta 52 (2007) 2950–2958.
[19] L. Zhang, X.B. Chen, S.P. Jiang, H.Q. He, Y. Xiang, Solid State Ionics 180 (2009) 1076–1082.
[20] A.B. Munoz-Garcia, D.E. Bugaris, M. Pavone, J.P. Hodges, A. Huq, F.L. Chen, H.C. zur Loye, E.A. Carter, J. Am. Chem. Soc. 134 (2012) 6826–6833.

[21] A.B. Munoz-Garcia, M. Pavone, E.A. Carter, Chem. Mater. 23 (2011) 4525–4536.
[22] Z.L. Zhan, D. Han, T.Z. Wu, X.F. Ye, S.R. Wang, T.L. Wen, S. Cho, S.A. Barnett, RSC Adv. 2 (2012) 4075–4078.
[23] G.L. Xiao, Q. Liu, X.H. Dong, K. Huang, F.L. Chen, J. Power Sources 195 (2010) 8071–8074.
[24] D. Han, X.J. Liu, F.R. Zeng, J.Q. Qian, T.Z. Wu, Z.L. Zhan, Sci. Rep. 2 (2012).
[25] S.D. Park, J.M. Vohs, R.J. Gorte, Nature 404 (2000) 265–267.